

Investigation of the effect of eddy current artefacts in UTE-derived PET attenuation maps on PET reconstruction

Andrew Peter Aitken¹, Charalampous Tsoumpas¹, Daniel Giese¹, Sebastian Kozerke^{1,2}, Claudia Prieto¹, and Tobias Schaeffter¹

¹Division of Imaging Sciences and Biomedical Engineering, King's College London, London, London, United Kingdom, ²Institute for Biomedical Engineering, University and ETH Zurich, Zurich, Switzerland

Introduction: Deriving PET attenuation correction maps (AC maps) for use in hybrid PET-MR systems is challenging because no direct relation exists between PET attenuation coefficients (μ) and MR signal intensity. Segmented MRI has been used to assign appropriate μ values to each tissue class. Segmentation is difficult because bone and air both appear with little or no signal intensity in standard MRI, but have very different μ values. Ultrashort echo time (UTE) sequences can be used to distinguish between bone and air.^{1,2} However, these sequences require sampling to be performed while the gradients are ramped up, making them prone to eddy current artefacts.³ It has been shown that these artefacts lead to misclassifications in segmented AC maps⁴, particularly on the boundaries between soft tissue and air and between bone and soft tissue (Fig. 1), and that they can be corrected for by measuring the k-space trajectories using a magnetic field camera.⁴ In this study we investigate the effect of these misclassifications on simulated PET reconstructions.

Methods: MR data acquisition and AC map derivation: Dual echo UTE images were acquired of the head of two healthy volunteers (3T Philips, TE1/TE2/TR = 0.14/2.14/4.7ms, 1.3mm³ isotropic voxel size, 250mm FOV). The k-space trajectories were measured during a separate calibration scan using a dynamic magnetic field camera⁵ (Skopec LLC, Zurich, CH), as described in Ref 4. Images were reconstructed first using nominal k-space trajectories and again using measured k-space trajectories. Both sets of images were segmented to produce segmented AC maps (AC_{meas} & AC_{nom}).⁴ **PET simulation:** PET data were simulated as illustrated in Fig. 2, using the STIR package.⁶ A simulated emission map was derived by using a combination of the bone, air and soft tissue segmentations from AC_{meas} and the CSF, white matter and gray matter segmentations from the BrainWeb atlas.⁷ Three simulated spherical lesions of 20 mm diameter were then added. The resulting segmentation was assigned appropriate emission values and smoothed before being forward projected to produce a 3D reference sinogram. Three PET reconstructions were performed, using a 3D OSEM algorithm.⁶ A reference image (PET_{ref}) was reconstructed from the reference sinogram, with no simulation or correction for attenuation or scatter effects. Attenuation coefficient factors and scatter estimates derived from AC_{meas} were then used to produce an attenuated sinogram with scatter from the reference sinogram. Reconstruction of this sinogram was achieved using attenuation and scatter corrections using μ and scatter estimates derived from AC_{meas} and again from AC_{nom} , to generate images PET_{meas} and PET_{nom} , respectively. Poisson noise was added to each sinogram before reconstruction.

Results: Reconstructed PET images for each case, overlaid on the MR images are shown in Fig.3 for one subject. Relative difference maps are also shown between PET_{nom} and PET_{ref} , between PET_{meas} and PET_{ref} and between PET_{nom} and PET_{meas} . In PET_{nom} , mean uptake in the brain was over-estimated by 9.16% compared to PET_{ref} . The corresponding value between PET_{meas} and PET_{ref} was 0.34%. The largest errors in PET_{nom} occurred in the posterior and superior regions of the brain, where large regions of misclassified bone appear in the AC maps. In these regions the relative difference tended to ~25% close to the skull. Maximum and mean relative differences of standardized uptake value (SUV) for each lesion are shown in Table 1.

Conclusions: Misclassifications in UTE-derived PET AC maps due to eddy current artefacts lead to regional errors in measured SUV in simulated PET images of up to 25%. In simulated lesions, uptake was overestimated by up to 12.19%. When eddy currents were corrected for in the UTE reconstruction using k-space trajectories measured with a magnetic field camera, errors in the simulated PET reconstruction were greatly reduced, with the maximum error in simulated regions within 2.13% of a reference reconstruction.

Table 1- Quantification of SUV error in simulated lesions

	$(PET_{nom} - PET_{ref}) / PET_{ref} \times 100\%$		$(PET_{meas} - PET_{ref}) / PET_{ref} \times 100\%$	
	Mean	Max	Mean	Max
Lesion 1	4.15%	7.17%	-0.21%	-2.13%
Lesion 2	10.25%	10.51%	0.86%	1.11%
Lesion 3	11.3%	12.19%	-0.46%	1.81%

Table 1- Quantification of SUV error in simulated lesions

	$(PET_{nom} - PET_{ref}) / PET_{ref} \times 100\%$		$(PET_{meas} - PET_{ref}) / PET_{ref} \times 100\%$	
	Mean	Max	Mean	Max
Lesion 1	4.15%	7.17%	-0.21%	-2.13%
Lesion 2	10.25%	10.51%	0.86%	1.11%
Lesion 3	11.3%	12.19%	-0.46%	1.81%

References: [1] Catana 2010 JNM 51:1431-8 [2] Keereaman et al. 2010 JNM 51:812-18 [3] Atkinson et al. 2009 MRM 62:532-7 [4] Aitken et al. 2012 ESMRMB 238 [5] Barmet et al. 2008 MRM 60:187-97 [6] Thielemans et al. 2012 PMB 57:867-83 [7] Aubert-Broche et al. 2006 NeuroImage 32:138-45

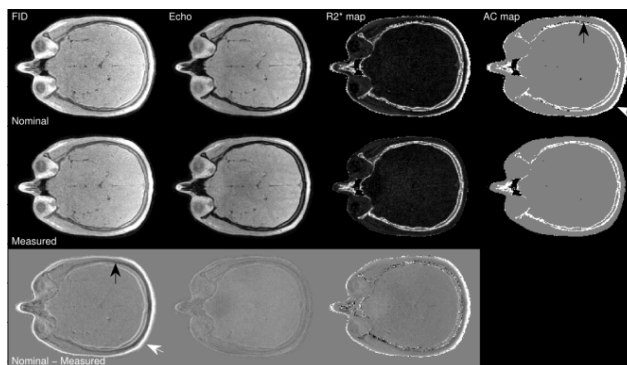


Figure 1 – Dual echo UTE images reconstructed with nominal k-space trajectories and with trajectories measured with a magnetic field camera, along with derived R_2^* maps and segmented AC maps. Arrows indicate misclassifications when nominal trajectories are used.

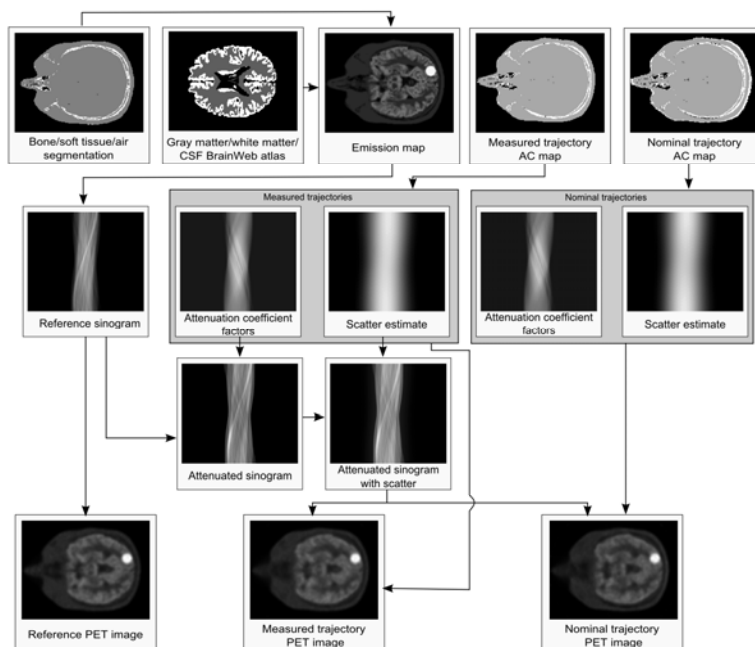


Figure 2 – PET simulation workflow to generate 3 PET reconstructions: i) reference image (no μ or scatter), and using μ and scatter from ii) AC_{meas} and iii) AC_{nom} .

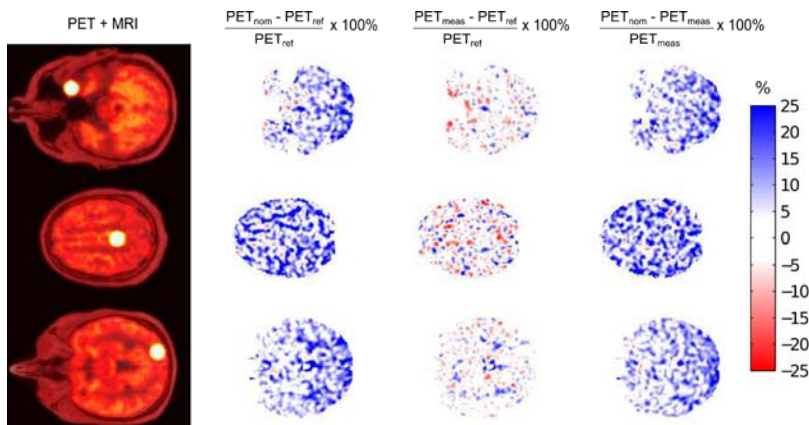


Figure 3 – Difference maps for simulated PET images. Mean uptake is overestimated by 9.16% with PET_{nom} and only by 0.34% with PET_{meas} .